


# Very massive stars in not so massive clusters

Seungkyung Oh<sup>1,2</sup>  and Pavel Kroupa<sup>1,3</sup>

<sup>1</sup>*Helmholtz-Institut für Strahlen- und Kernphysik (HISKP), University of Bonn, Nussallee 14-16, 53115 Bonn, Germany*

<sup>2</sup>*Department of Physics and Astronomy, University of Sheffield, Hicks Building, Hounsfield Road, Sheffield S3 7RH, UK*

<sup>3</sup>*Faculty of Mathematics and Physics, Astronomical Institute, Charles University in Prague, V Holešovičkách 2, CZ-180 00 Praha 8, Czech Republic*

Accepted Received

## ABSTRACT

Very young star clusters in the Milky Way exhibit a well-defined relation between their maximum stellar mass,  $m_{\max}$ , and their mass in stars,  $M_{\text{ecl}}$ . A recent study shows that the young intermediate-mass star cluster VVV CL041 possibly hosts a  $\gtrsim 80 M_{\odot}$  star, WR62-2, which appears to violate the existence of the  $m_{\max}-M_{\text{ecl}}$  relation since the mass of the star is almost two times higher than that expected from the relation. By performing direct  $N$ -body calculations with the same mass as the cluster VVV CL041 ( $\approx 3000 M_{\odot}$ ), we study whether such a very massive star can be formed via dynamically induced stellar collisions in a binary-rich star cluster that initially follows the  $m_{\max}-M_{\text{ecl}}$  relation. Eight out of 100 clusters form a star more massive than  $80 M_{\odot}$  through multiple stellar collisions. This suggests that the VVV CL041 cluster may have become an outlier of the relation because of its early-dynamical evolution, even if the cluster followed the relation at birth. We find that more than half of our model clusters host a merger product as its most massive member within the first 5 Myr of cluster evolution. Thus, the existence of stars more massive than the  $m_{\max}-M_{\text{ecl}}$  relation in some young clusters is expected due to dynamical processes despite the validity of the  $m_{\max}-M_{\text{ecl}}$  relation. We briefly discuss evolution of binary populations in our model.

**Key words:** methods: numerical – stars: kinematics and dynamics – stars: massive – open clusters and associations: general – open clusters and associations: individual: VVV CL041 – galaxies: star clusters: general

## 1 INTRODUCTION

Very young ( $\lesssim 4$  Myr) star clusters in the Milky way show a well defined relation between the mass of the most massive star in the cluster,  $m_{\max}$ , and the cluster mass in stars,  $M_{\text{ecl}}$  (Fig. 1). That is, the maximum stellar mass in a very young cluster appear to be determined by the cluster mass, i.e. by the given mass budget (Weidner, Kroupa & Pfamm-Altenburg 2013 and references therein). The relation has only a small spread and argues against the random sampling of stellar masses from an initial mass function (IMF) with a universal stellar upper mass limit (Elmegreen 2006; Selman & Melnick 2008). Noteworthy here are the homogeneous surveys by Kirk & Myers (2011, 2012) of low-mass very young clusters and by Stephens et al. (2017) with the *Hubble Space Telescope* (*HST*) of previously thought isolated massive young stellar objects (MYSOs) in the Large Magellanic Cloud (LMC). We emphasize that the Kirk & Myers (2011, 2012) data and the Stephens et al. (2017) data are from a homogeneous surveys performed by the same teams using

the same methods and telescopes. Especially noteworthy is the Stephens et al. (2017) study that targeted seven MYSOs in the LMC which were thought to be, based on *Spitzer* observations, single stars formed in isolation. Stephens et al. found, with their *HST* data, very compact massive clusters at the positions of these seven stars, with all seven being very close to the  $m_{\max}-M_{\text{ecl}}$  relation. Both teams show their data to be in excellent agreement with the  $m_{\max}-M_{\text{ecl}}$  relation. In their VVV survey of young star clusters Ramírez Alegría et al. (2016) find the clusters, which are a few Myr older than those in the Stephens et al. and Kirk & Myers (2011, 2012) surveys, to also follow the  $m_{\max}-M_{\text{ecl}}$  relation.

Some recent efforts to find massive stars in the Galaxy have led to discoveries of young (relatively massive) star clusters and massive star contents in them (e.g. Berkeley 90; Maíz Apellániz et al. 2015; VVV CL041; Chené et al. 2015). The masses of these clusters are only about  $2000-3000 M_{\odot}$ , but they host massive stars ( $\gtrsim 70 M_{\odot}$ ) that are heavier than the value ( $\approx 40 M_{\odot}$ ) given by the empirical  $m_{\max}-M_{\text{ecl}}$  relation of Weidner et al. (2013). Thus these clusters may question the existence of the physical  $m_{\max}-M_{\text{ecl}}$  relation with a small intrinsic dispersion.

\* E-mail: s.oh@sheffield.ac.uk

The present-day values of  $m_{\max}$  and  $M_{\text{ecl}}$  can be different from those at the clusters' birth because of (dynamical) evolutionary processes, such as dynamical ejections and stellar collisions. [Oh & Kroupa \(2012\)](#) investigated if the evolutionary processes can alter the relation significantly, in particular focusing on ejections, and they conclude that the processes do not change the global relation. But they also show that, at 3 Myr, a high proportion of moderately massive star clusters ( $M_{\text{ecl}} = 10^{3.5}\text{--}10^4 M_{\odot}$ , their most massive star-cluster models) can have their most massive star being affected by stellar mergers.

Stellar mergers have been considered to be one possible channel to form a massive star. Especially, in a dense star cluster, collisions can be triggered by few-body close encounters, and furthermore even runaway collisions can occur. Stellar collisions play an important role in forming exotic objects, in star clusters particularly, such as blue stragglers (e.g. [Hills & Day 1976](#); [Lombardi et al. 1996](#); [Sills et al. 2001](#)), B[e] stars (e.g. [Jeřábková et al. 2016](#)), red novae (e.g. [Tylenda & Kamiński 2016](#)), and stars with mass  $\gtrsim 200 M_{\odot}$  (e.g. [Banerjee, Kroupa & Oh 2012](#)). Previous studies have shown that very massive stars form in young, dense (massive) star clusters via stellar mergers, either including primordial binaries ([Banerjee et al. 2012](#)) or through a purely close three-body interaction ([Gaburov et al. 2008](#)).

In this study, we investigate whether  $3000 M_{\odot}$  star clusters that initially follow the  $m_{\max}\text{--}M_{\text{ecl}}$  relation can host stars with masses  $\gtrsim 80 M_{\odot}$  during their evolution as a result of stellar collisions in the clusters. In Section 2 our  $N$ -body model is described. Section 3 presents our results showing that (very) massive stars ( $\gtrsim 80 M_{\odot}$ ) can form via mergers within the first few Myr of the evolution of the cluster. This is in particular the case for clusters as massive as VVV CL041, even though initially such clusters do not host a star more massive than  $\approx 43 M_{\odot}$ . We also document the evolution of cluster size and binary populations for our model clusters in Section 3. The discussion and summary follow in Section 4.

## 2 N-BODY MODEL

We model the first 5 Myr evolution of VVV CL041-like clusters with the direct  $N$ -body code, NBODY6 ([Aarseth 2003](#)). The estimated age and mass of the VVV CL041 cluster are respectively 1–4 Myr and  $(3 \pm 2) \times 10^3 M_{\odot}$  ([Chené et al. 2015](#)). We set the initial mass of our gas-free model clusters,  $M_{\text{ecl}}$ , to be  $3000 M_{\odot}$  which is close to the observationally estimated mass. We note that the true initial mass of the cluster could have been higher because of the possible loss of stars as a result of residual-gas expulsion (e.g. [Kroupa, Aarseth & Hurley 2001](#); [Brinkmann, Banerjee, Motwani & Kroupa 2017](#)). If so then this work presents a conservative estimate because more massive and thus denser clusters lead to more stellar mergers. The initial half-mass radius is set to be 0.28 pc following the relation between the initial half-mass radius and cluster mass,  $r_h(0) = 0.1 \times (M_{\text{ecl}}/M_{\odot})^{0.13}$  ([Marks & Kroupa 2012](#)). This is consistent with the survey by [Testi et al. \(1997\)](#). Dynamical evolution expands the size of model clusters to an average half-mass radius,  $r_h$ , of about 0.8 pc at 5 Myr as a result of dynamical evolution (Section 3.2). Initial positions and velocities of the stellar systems (binaries and single stars) follow the Plummer phase-space density dis-

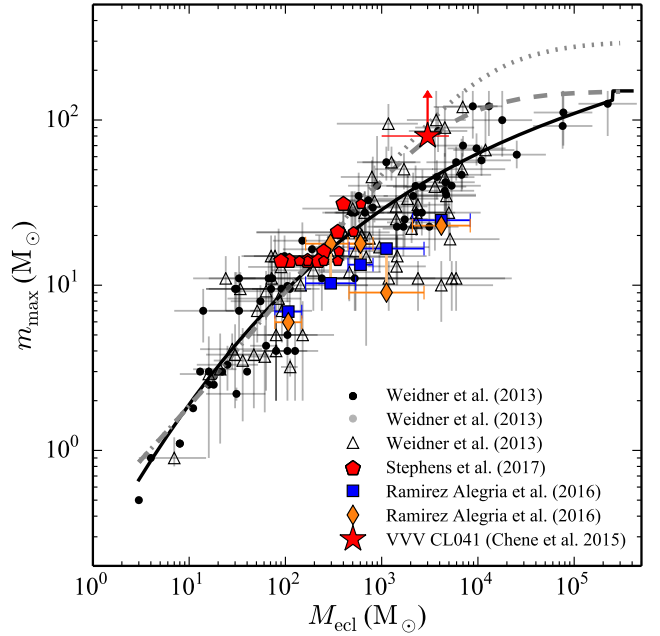


**Figure 1.** Embedded star-cluster mass versus maximum stellar mass from [Weidner et al. \(2013\)](#). The black circles are the low-error sub-sample clusters that are used to obtain the fitted relation (black solid line, equation 1 in [Weidner et al. 2013](#)), while open triangles are the clusters that are excluded from fitting because of their high uncertainty. The red star marks  $m_{\max}$  and  $M_{\text{ecl}}$  values of VVV CL041 from [Chené et al. \(2015\)](#). The blue squares and orange diamonds are two different mass estimates of  $m_{\max}$  stars in clusters studied by [Ramírez Alegría et al. \(2016\)](#). The red pentagons are seven isolated MYSOs in the LMC and stellar clusters around them ([Stephens et al. 2017](#)). The large and small symbols are the estimated cluster masses using 1 and 2.5 Myr isochrones, respectively ([Stephens et al. 2017](#)). The dashed and dotted lines are the semi-analytical relation in WK06 assuming the upper stellar-mass limit to be 150 and  $300 M_{\odot}$ , respectively.

tribution under the assumption that the cluster is initially in virial equilibrium. The model clusters are initially fully mass-segregated ([Plunkett et al. 2018](#)) by using the method in [Baumgardt, De Marchi & Kroupa \(2008\)](#) in which the more massive stars are more bound to a cluster. We note that the mass-segregation time-scale of O stars in unsegregated clusters with our model cluster parameters is only  $\lesssim 0.2$  Myr ([Oh & Kroupa 2016](#)) and thus results from initially non-segregated clusters would not be much different from those from the initially segregated ones. We carried out 100 realisations with different random seed numbers.

We aim to test whether a cluster initially on the  $m_{\max}\text{--}M_{\text{ecl}}$  relation can have a star more massive than  $m_{\max}$  through dynamical evolution. The initial mass of the most massive star is, thus, assigned to be the value derived from the  $m_{\max}\text{--}M_{\text{ecl}}$  relation, equation (1) in [Weidner et al. \(2013\)](#), which is a third-order polynomial fit to the observed cluster samples (Fig. 1). For a cluster with  $M_{\text{ecl}} = 3000 M_{\odot}$ , the relation gives  $m_{\max} = 43.14 M_{\odot}$ .

The initial masses of stars in a cluster are drawn by using a modified version of the optimal sampling method ([Kroupa et al. 2013](#)), which divides a cluster mass into individual stellar masses following the exact form of the canon-

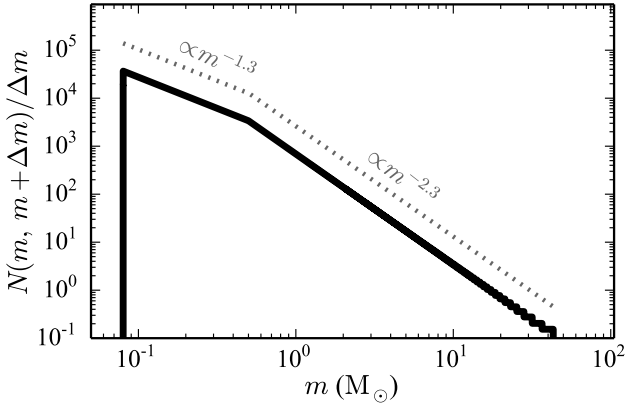


**Figure 2.** Initial mass function of our model. In this figure,  $N(m_i, m_i + \Delta m_i) = 1$  and  $\Delta m_i = (m_{i-1} + m_i)/2 - (m_i + m_{i+1})/2$ , where  $i = 3, \dots, N-1$  (see also equations 3 and 4). The upper and lower boundaries are set to be  $m_1 = m_{\max}$  and  $0.08 M_{\odot}$ , respectively. Note that optimal sampling eliminates Poisson scatter.

ical initial mass function (IMF),

$$\xi(m) = k \begin{cases} \left(\frac{m}{0.5}\right)^{-\alpha_1}, & 0.08 \leq m/M_{\odot} \leq 0.5, & \alpha_1 = 1.3, \\ \left(\frac{m}{0.5}\right)^{-\alpha_2}, & 0.5 \leq m/M_{\odot} \leq m_{\max}, & \alpha_2 = 2.3. \end{cases} \quad (1)$$

The normalisation constant  $k$  in equation (1) is deduced from

$$M_{\text{ecl}} - m_{\max} = \int_{m_{\text{lim}}}^{m_{\max}} m \xi(m) dm, \quad (2)$$

where the function  $m_{\max}(M_{\text{ecl}})$  is given by equation (1) in Weidner et al. (2013), and the lower mass limit  $m_{\text{lim}} = 0.08 M_{\odot}$ . The stellar upper and lower mass boundaries ( $m^{\text{up}}$  and  $m^{\text{low}}$ , respectively) between which there exists exactly one star follow from

$$1 = \int_{m_i^{\text{low}}}^{m_i^{\text{up}}} \xi(m) dm, \quad \text{where } i = 2, 3, \dots, N, \quad (3)$$

where  $m_2^{\text{up}} = m_{\max}$  and  $m_i^{\text{up}} = m_{i-1}^{\text{low}}$ . With these boundaries, masses of individual stars are generated as

$$m_i = \int_{m_i^{\text{low}}}^{m_i^{\text{up}}} m \xi(m) dm, \quad (4)$$

until the total mass of stars reaches the cluster mass (see also Schulz, Pflamm-Altenburg & Kroupa 2015 for more details on improved optimal sampling). For a  $3000 M_{\odot}$  cluster, in total  $N = 5438$  stars are obtained, including the  $m_{\max}$  star. The mean stellar mass is  $\approx 0.55 M_{\odot}$ . The initial stellar mass function of the  $3000 M_{\odot}$  cluster is presented in Fig. 2. It is noteworthy that optimal sampling produces a unique set of stellar masses for a given cluster mass (see also Yan, Jerabkova & Kroupa 2017). Thus all clusters modelled here have the same set of initial stellar masses while other initial conditions of the stars, such as the positions, velocities, and orbital parameters of binaries, vary in each realisation with a different random number seed.

We assume the initial binary fraction to be unity, which is all stars are initially in a binary system. This comes about because binary-star formation must be the vastly dominant

outcome of star formation rather than higher-order multiple systems (Goodwin & Kroupa 2005). Furthermore, the results of Sana et al. (2014) suggest that massive stars form nearly exclusively in multiple systems. We use separate orbital-parameter distributions for high-mass (primary mass  $m_p \geq 5 M_{\odot}$ ) and lower mass ( $m_p < 5 M_{\odot}$ ) binaries as observations indicate that they have different distributions (e.g. Duquennoy & Mayor 1991 for solar-mass binaries and Sana et al. 2012; Kobulnicky et al. 2014 for O-star binaries). To model realistic massive binary populations, we adopt the initial period distribution from Sana et al. (2012) for massive ( $m_p \geq 5 M_{\odot}$ ) binaries that is derived from observations of O-star binaries in young open star clusters in the Galaxy. The distribution has the form of  $f(\log_{10} P) \propto (\log_{10} P)^{-0.55}$ , where the period  $P$  is in d. We chose a period range  $0.15 \leq \log_{10}(P/d) \leq 6.7$  (Oh et al. 2015). Short period massive binaries are found to be on a circular orbit (e.g. Kiminki & Kobulnicky 2012; Sana et al. 2012). We put massive binaries with  $P \leq 2$  d in a circular orbit with an eccentricity ( $e$ ) of 0, while for the binaries with  $P > 2$  d, their eccentricities are set to be drawn from the uniform distribution with a range  $0 \leq e \leq 0.6$  similar to observations (Kiminki & Kobulnicky 2012; Sana et al. 2012). Mass ratios of the observed O-star binaries can be approximated by a uniform distribution (Sana et al. 2012; Kobulnicky et al. 2014). To achieve the uniform mass-ratio distribution while keeping the canonical IMF unchanged, the secondary masses of massive star binaries are picked from the stellar masses already drawn from the IMF, with the closest mass ratio to a value drawn from a uniform distribution with  $0.1 \leq q \leq 1.0$  (Oh & Kroupa 2016). For lower mass binaries ( $m_p < 5 M_{\odot}$ ), the initial period and eccentricity distributions are equation (8) of Kroupa (1995b) and the thermal distribution,  $f(e) = 2e$ , respectively. Their components are randomly paired from the IMF. In this work we do not take into account pre-main-sequence eigevolution which establishes, during the early pre-main-sequence phase, the observed correlation between orbital period, eccentricity, and mass ratio for late-type binary systems (Kroupa 1995a; Belloni et al. 2017). We note that the possibility of a merger product to become the most massive star in a cluster is almost twice as high in initially binary-rich cluster models than in single star cluster models (see table 3 in Oh & Kroupa 2012).

The distribution of initial binding energies of the binaries is shown in Fig. 3. The binding energy of a binary,  $E_b$ , is

$$E_b = -G \frac{m_p m_s}{2a}, \quad (5)$$

where  $G$ ,  $m_s$ , and  $a$  are the gravitational constant, secondary mass, and semimajor axis of a binary, respectively. In total, the binaries in the model clusters have a binding energy of  $\approx -5.6 \times 10^6 M_{\odot} \text{pc}^2 \text{Myr}^{-2}$  on average. For a cluster in virial equilibrium, its total energy,  $E_{\text{tot,cl}}$ , is

$$E_{\text{tot,cl}} = E_P + E_K = -E_K, \quad (6)$$

where  $E_P$  and  $E_K$  are the total potential and kinetic energy of the cluster, respectively. For the Plummer model, this can be obtained as

$$E_{\text{tot,cl}} = -\frac{3\pi}{64} \frac{GM_{\text{ecl}}^2}{r_p}, \quad (7)$$

where  $r_p$  is the Plummer radius,  $\approx 0.776 r_h$  (Heggie & Hut

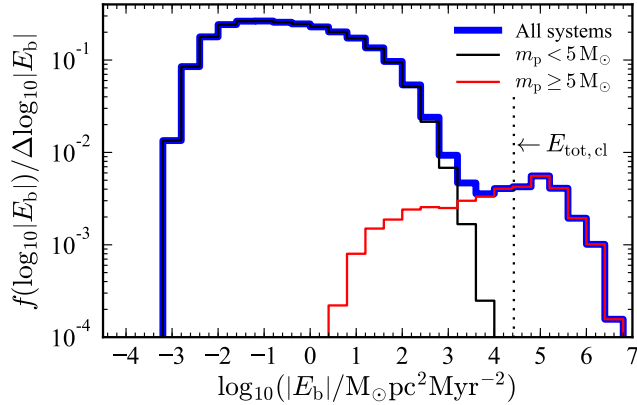


**Figure 3.** Initial binary binding energy distribution. The blue thick line presents the distribution of all binary systems. The black thin line is the energy distribution of low-mass binaries ( $m_p < 5 M_\odot$ ) while the red thin line shows the distribution of massive binaries ( $m_p \geq 5 M_\odot$ ). They are averaged for 100 cluster models. The vertical dotted line indicates the total energy of the cluster.

2003). For our cluster model,  $E_{\text{tot,cl}} \approx -2.7 \times 10^4 M_\odot \text{pc}^2 \text{Myr}^{-2}$  and its absolute value is in good agreement of the total kinetic energy of our model clusters. This shows that an extremely high energy is initially stored in binary systems compared to the total cluster energy. The systems in the high energy tail in Fig. 3,  $\log_{10}(|E_b|/M_\odot \text{pc}^2 \text{Myr}^{-2}) \geq 4.5$ , which are massive short-period binaries, indicate that a single binary can hold energy larger than the entire cluster energy (see also Leonard & Duncan 1988). Examples are massive binaries with a period of a few days in the Sana et al. (2012) samples. For instance, the binding energy of CPD-592603, a spectroscopic binary system in Trumpler 16, is  $\approx 1.3 \times 10^6 M_\odot \text{pc}^2 \text{Myr}^{-2}$  based on its orbital parameters in Rauw et al. (2001,  $P = 2.15 \text{d}$ ,  $m_p \sin^3 i = 22.1 M_\odot$ , and  $m_s \sin^3 i = 14.1 M_\odot$ ), while the total energy of its parent cluster, Trumpler 16, is  $< 1.7 \times 10^5 M_\odot \text{pc}^2 \text{Myr}^{-2}$  obtained by assuming a cluster mass of  $10^4 M_\odot$  and a size of 0.5 pc (equation 6).<sup>1</sup>

Stellar evolution is incorporated in the code with single and binary stellar evolution libraries (Hurley, Pols & Tout 2000; Hurley, Tout & Pols 2002). We assume solar metallicity  $Z = 0.02$  for our models. By activating the stellar evolution option, the  $N$ -body code allows two stars to merge when the (pericentre) distance between them is smaller than the sum of their radii. No mass-loss is assumed in the merger procedure, unless the kinetic energy of the system exceeds the absolute value of binding energy of the secondary star, in which case 30 per cent of the present-day secondary star mass is removed (Aarseth 2003). After they merge, they are internally completely mixed. The age of the merger product is assigned based on the amount of hydrogen in the core. Then the star evolves following the normal stellar evolution recipe for the corresponding stellar mass (see also Baner-

<sup>1</sup> The cluster parameters of Trumpler 16 are not well-constrained. We adopt cluster parameters for Trumpler 16 from its neighbour cluster Trumpler 14 (Portegies Zwart, McMillan & Gieles 2010) which is similar to Trumpler 16 but younger and richer.

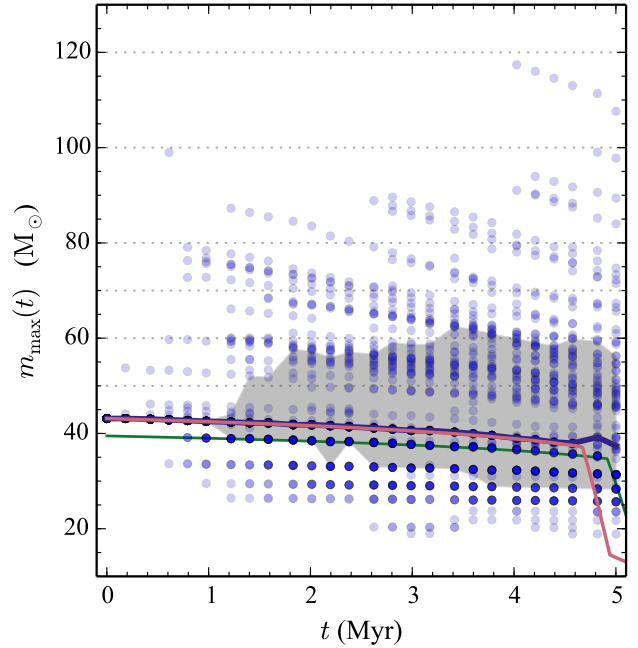


**Figure 4.** Present-day mass of the most massive star within 1 pc radius of the model clusters,  $m_{\text{max}}(t)$ , as a function of time (blue circles). Horizontal dotted lines indicate masses of 50, 60, 70, 80, 100, and 120  $M_\odot$  (from bottom to top). Red and green lines are the evolutionary tracks of stars with initial masses of 43.14 and 39.49  $M_\odot$  that are initially the most and the second-most massive stars in the cluster,  $m_1(t)$  and  $m_2(t)$ , respectively. The thick blue line, which mostly overlaps with the evolutionary track of  $m_1$  (i.e.  $m_{\text{max}}(t=0)$ ), is the median  $m_{\text{max}}(t)$  of 100 cluster models. The grey shaded area indicates the central 68 percentile.

jee, Kroupa & Oh 2012 for more discussions on the merger procedure of the code).

Recent numerical studies (Suzuki et al. 2007; Glebbeek et al. 2013) on the evolution of massive merger products from two massive stars show that the mass-loss during a collision is rather small, 8–10 per cent, and that the merger products evolve similarly to normal single stars with the same mass. Thus the recipe used in the code (e.g. no mass-loss and normal stellar evolution) may not be far from reality. These studies also show the merger products to have slightly larger sizes and higher luminosities than normal single stars with the same mass.

### 3 RESULTS

In this section, we present the collisional products that are more massive than 80  $M_\odot$  formed via multiple stellar collisions (Section 3.1) and the evolution of cluster size and binary properties (Section 3.2).

#### 3.1 Formation of massive stars through dynamical stellar collisions

Stars in a cluster gravitationally interact with each other. Particularly close encounters can lead stars/binaries to

merge or to be ejected from their birth cluster. The encounter rate, i.e. the number of encounters of a star/system per unit time per unit volume, is given by  $n\sigma v_{\text{rel}}$ , where  $n$  is a stellar number density,  $\sigma$  the encounter cross section, and  $v_{\text{rel}}$  is the mean relative speed. The cross section is

$$\sigma = \pi r_{\text{min}}^2 \left( 1 + \frac{2GM_{\text{enc}}}{r_{\text{min}}v_{\text{rel}}^2} \right), \quad (8)$$

where  $r_{\text{min}}$  is the minimum distance and  $M_{\text{enc}}$  is the sum of the binary mass and the mass of the star/system that the binary encounters. The second term on the right side of equation (8) is gravitational focusing. For a single star,  $r_{\text{min}}$  is approximately the radius of the star. For a binary,  $r_{\text{min}}$  is the semi-major axis of the binary  $a$ . For a Maxwellian velocity distribution,  $v_{\text{rel}}$  is  $\sqrt{2}\sigma_{\text{ecl}}$  (Leonard 1989) where  $\sigma_{\text{ecl}}$  is the characteristic velocity dispersion of the cluster,  $\sigma_{\text{ecl}} \approx 0.88^2 GM_{\text{ecl}}/r_{\text{h}}$  (Kroupa 2008). For the close encounter cross section of a hard binary, the gravitational focusing term in equation (8) is dominant. The close encounter rate of a binary can be written as

$$\Gamma = \sqrt{2}\pi G \frac{naM_{\text{enc}}}{\sigma_{\text{ecl}}}. \quad (9)$$

For our model clusters the initial number density of systems within the half-mass radius and  $\sigma_{\text{ecl}}$  are  $\approx 1.5 \times 10^3 \text{ pc}^{-3}$  and  $4.2 \text{ km s}^{-1}$ , respectively. For simplicity, we assume the typical mass of a system that a binary encounters to be  $2 \times \bar{m}$ , where  $\bar{m} = 0.55 M_{\odot}$  is the mean stellar mass in our model clusters as we initially have only binaries in our models. The close encounter rate of an equal mass binary of  $20 M_{\odot} + 20 M_{\odot}$  with a semimajor axis of 1 au in our model cluster is approximately  $0.014 \text{ pc}^{-3} \text{ Myr}^{-1}$ . The total number of encounters that occur in a cluster can be estimated by multiplying the number densities of binaries to their encounter rate and summing up all the number of encounters for different binaries. However this is difficult to calculate because of a large variation in parameters, such as  $M_{\text{enc}}$ ,  $a$ , and densities of individual object types. A fraction of close encounters result in stellar collisions. On average, for our model about 11 stellar collisions occur in a cluster during the first 5 Myr evolution. Among them, about 5 collisions are mergers of binaries with a highly eccentric orbit at  $t = 0 \text{ Myr}$  and the majority of them are low-mass binaries (see Section 3.2). About 6 collisions are dynamically induced in a cluster, on average.

Stellar collisions or dynamical ejections of the most massive star change the mass of the most massive star as a cluster evolves. We obtain the present-day mass of the most massive star,  $m_{\text{max}}(t)$ , within a 1 pc radius of the model clusters at time  $t$ . In Fig 4, we plot  $m_{\text{max}}(t)$  of all model clusters for every 0.2 Myr of the first 5 Myr evolution. The points above the red line (mass evolution of the  $m_{\text{max}}$  star) in Fig. 4 are products of stellar collisions within the cluster while those below the red line before  $\approx 4.7 \text{ Myr}$  indicate that dynamical ejection of the most massive star occurred in these clusters. Our model clusters all have the same  $m_{\text{max}}$  star at the beginning (Section 2). There is no change of the most massive star for more than 68 per cent of the clusters until an age of 1 Myr. As the clusters evolve, stellar collisions and dynamical ejections produce a spread in  $m_{\text{max}}(t)$  over a large range of stellar mass after 1 Myr. The median value of  $m_{\text{max}}(t)$  (thick blue line in Fig. 4) falls on top of the evolution track of the  $m_1 = m_{\text{max}}(t = 0)$  star (red line in Fig. 4) until 4.6 Myr, at

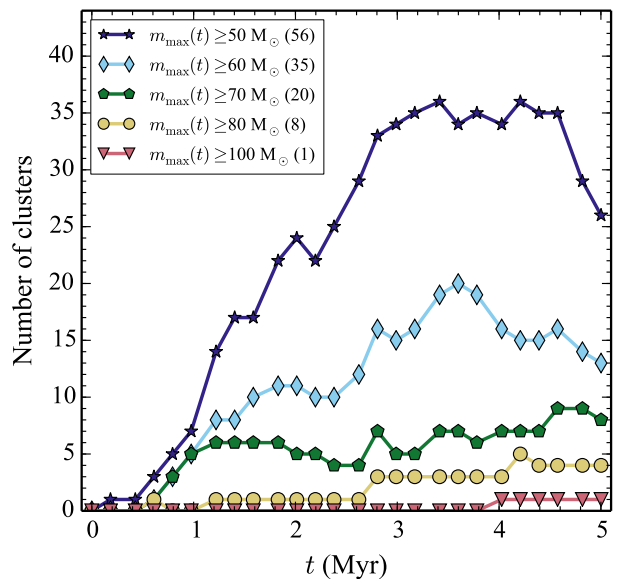


**Figure 5.** Number of clusters in an ensemble of 100 clusters in which the present-day maximum stellar mass,  $m_{\text{max}}(t)$ , is larger than 50, 60, 70, 80, and  $100 M_{\odot}$  as a function of time. Numbers in the legend indicate the total number of clusters which produce  $m_{\text{max}}(t)$  larger than 50, 60, 70, 80, and  $100 M_{\odot}$  within the first 5 Myr of evolution. Solid lines simply connect points of each groups.

which time the  $m_1$  star enters the Hertzsprung gap and starts losing its mass significantly. Thereafter, the median value is higher than the evolved mass of  $m_2$  (green line in Fig. 4) which is the most massive star at the time, if only the single stellar evolutionary effect is accounted for (i.e. without any dynamical evolution and binary merger). This implies that later than 4.6 Myr in more than 50 per cent of  $\approx 3000 M_{\odot}$  clusters, the most massive star is a merger product.

We note that only the very first collisional products that appear at 0.2 Myr in Fig. 4 are purely due to a small orbital separation of the initial binaries. The mergers that occur later than 0.2 Myr are mostly induced by perturbations from other stars through few-body close encounters; that is the encounters increase the eccentricity and thus decrease the pericentre distance of the binary systems.

In Fig. 5 is shown the number of clusters whose most massive star has a mass higher than  $50 M_{\odot}$  at a given time. More than 30 per cent of the clusters host a star more massive than  $50 M_{\odot}$ , which is a merger product, between 2.5 and 4.5 Myr (Fig. 5). The cluster number decreases at several points because some have been dynamically ejected or have become less massive than the mass criteria used in Fig. 5 as a result of stellar evolution.

In our model clusters, the maximum stellar mass that can be generated by a collision of two stars is  $82.63 M_{\odot}$ , because the masses of the two most massive stars are  $43.14$  and  $39.49 M_{\odot}$  given by our stellar mass sampling. Our pairing method (close to giving a uniform mass-ratio distribution) rarely produce the system that is composed of the most massive star and the second massive star. In fact, only five such cases exist among the 100 realisations. Among them, only one case merged at about 4.4 Myr forming a  $74.1 M_{\odot}$  star. Thus, it is very unlikely that only a single collision

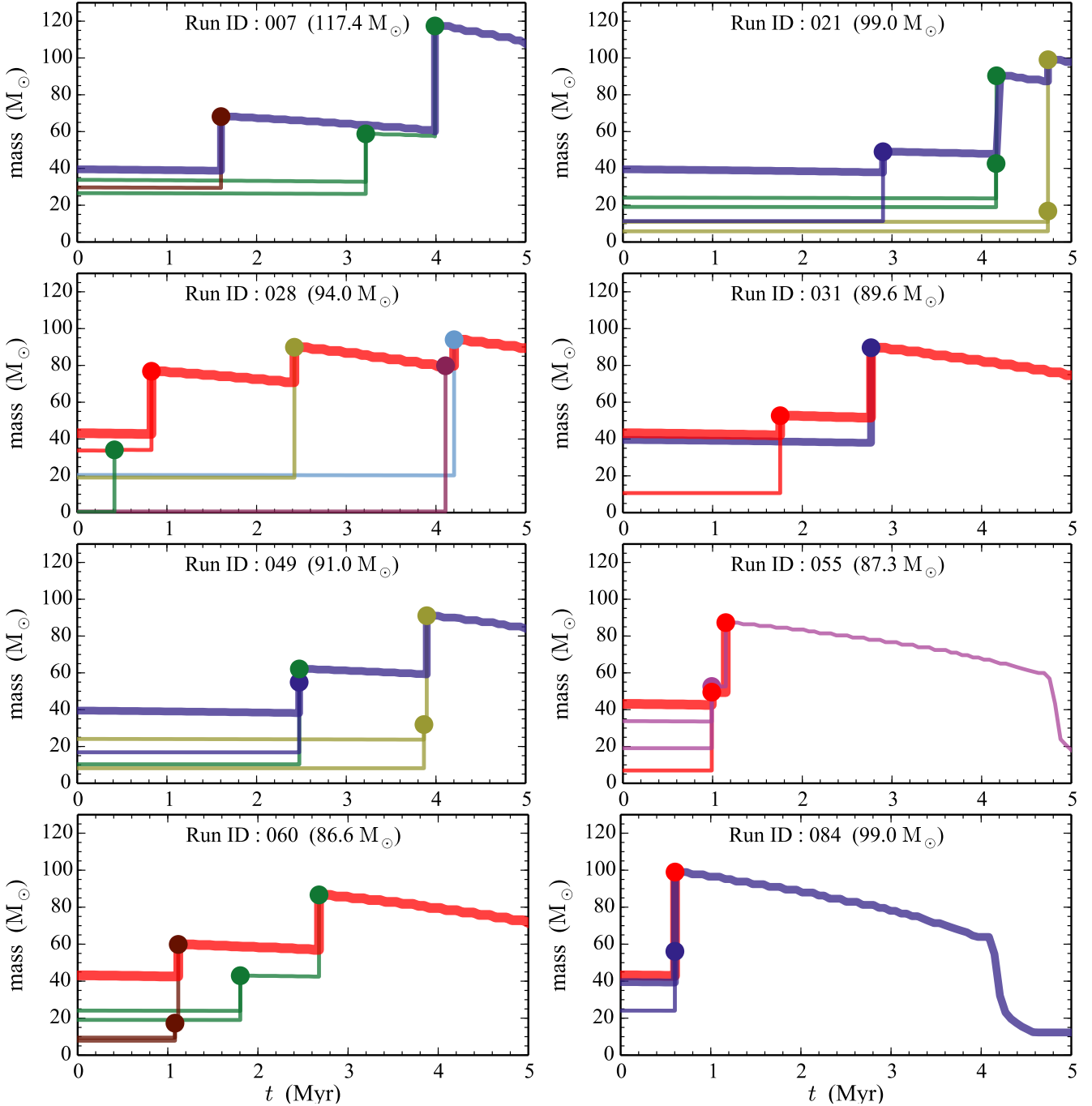


**Figure 6.** Collision history and mass evolution of stars that merge to  $m \geq 80 M_{\odot}$ . Masses of the final merger products at the time of last merger are written next to the run numbers. For Run 084, the star is dynamically ejected after the last collision (see Fig. 7). Each circle indicates a collision. Among stars involved in merging, initially the most massive ( $m_1$ ) and the second-most massive ( $m_2$ ) stars are indicated with a thick red- and a thick blue line, respectively. Two stars with the same colour imply that they are a natal pair.

via a binary merger forms a star more massive than  $80 M_{\odot}$  in a VVV CL041-like cluster under the assumption of the  $m_{\max} - M_{\text{ecl}}$  relation.

As shown in Figs 4–5, a few clusters produce a star with a mass above  $80 M_{\odot}$ , even a  $\approx 120 M_{\odot}$  star. Out of 100 model clusters, we find that eight clusters produce a star with  $m \geq 80 M_{\odot}$  through multiple stellar collisions within the first 5 Myr of cluster evolution, and among them one

cluster has formed a star with  $m \geq 100 M_{\odot}$ . Merger histories of these eight stars are plotted in Fig. 6. All these merger products experience at least two collision events. Two stars are products of five sequential merger events; that is, six stars become one star (Run IDs 021 and 028, Fig. 6). In general, only massive ( $> 5 M_{\odot}$ ) stars are involved in forming these massive stars. Only one (Run ID 028) out of eight cases shown in Fig. 6 takes two low-mass ( $0.4$  and  $0.6 M_{\odot}$ )

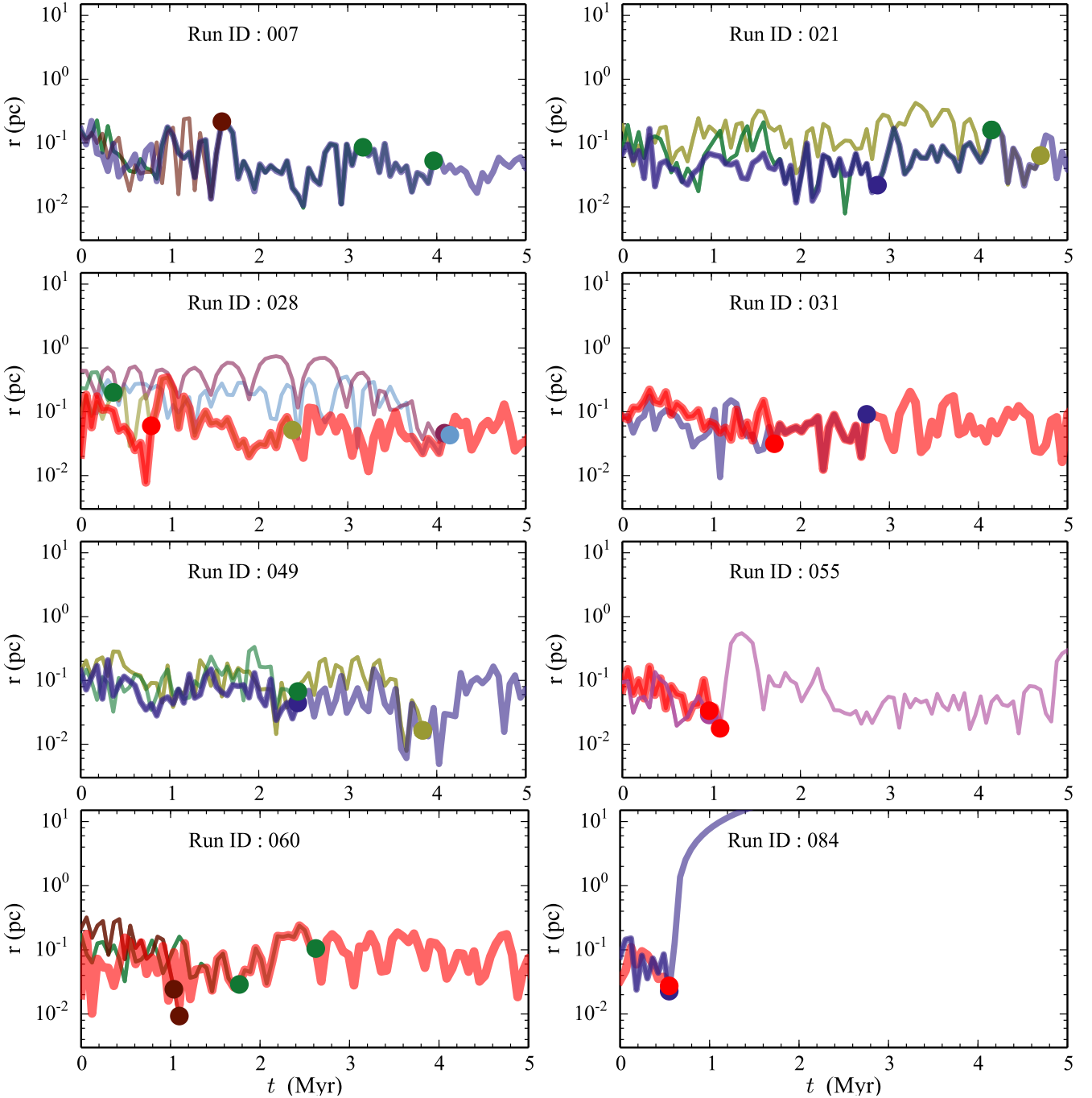


**Figure 7.** Locations of stars that form a star with  $m \geq 80 M_{\odot}$  as a function of time. The Y axis is the three dimensional distance,  $r$ , from the cluster centre. Filled circles show the location of the merger, as in Fig. 6.

stars. However, their mass is too small to contribute to the growth of the star.

We note that not all the merger products include the  $m_1$  (i.e. the  $m_{\max}$ ) star. Some of the very massive stars that are produced by stellar collisions do not include the initially most massive star. However, those that do not include the  $m_1$  star are formed from merger events that include the  $m_2$  star, i.e. the initially second-most massive star.

The radial distances from the cluster centre of stars that form  $>80 M_{\odot}$  stars in Fig. 6 are plotted in Fig. 7. Most of the

collisions occur within 0.1 pc of the cluster centre. They typically stay within the inner 0.3 pc. An exception is the merger product in Run ID 084. The star, that forms around 0.6 Myr and is ejected soon after its formation, has gone through two merger processes and dynamical ejection within a very short time. First, a binary–binary close encounter results in the merging of a binary, and then the merger product forms a close binary with the massive member of the other binary leaving the less massive star as a perturber to the inner close binary. The interaction in the triple system soon ejects

the lowest mass star (the perturber) and the inner close binary recoils in the opposite direction. As the last interaction hardens the close binary, the binary soon merges after the recoil.

In Fig. 7, an overlap of two or more lines indicates a multiple system. The figure shows that stars generally form a multiple system and move together before a collision occurs. In some cases, a binary merger and the formation of a new multiple system hosting the merged binary occur at the same time (e.g. Run IDs 028 and 031). This implies that the binary merger was induced by the new companion of the merged binary. Such a dynamically formed binary hosting the merger product can merge later by another close encounter with other stars. In the case of Run ID 028, a binary hosting the  $m_1$  star merges and the merged binary pairs with a  $19 M_{\odot}$  star at 0.8 Myr. The system remains as a binary for about 1.5 Myr and then the binary merges, probably induced by a dynamical interaction with another system. This massive star is in a multiple system over most of its lifetime, occasionally changing its companion through dynamical encounters, while it goes through several stellar mergers. Using similar  $N$ -body calculations to this study, Oh & Kroupa (2016) showed that massive merger products have a higher multiplicity fraction (see their fig. 12). This means that most massive merger products are likely found to be in a multiple system during the first few Myr of cluster evolution. Figure 7 also shows that dynamically formed massive multiple systems can remain as a high-order multiple system for a few Myr. For instance, in the Run ID 007 cluster, the  $m_2$  star and a massive binary form a triple system at  $\approx 0.8$  Myr, and then the system lasts for  $\approx 2.5$  Myr until the binary merges at 3.2 Myr, even though the  $m_2$  star merges with a  $29 M_{\odot}$  star at 1.6 Myr. We note that more stars can be involved in such multiple systems than those plotted in the figure, because only such stars that eventually merge to form the most massive star are plotted in the figure.

### 3.2 Evolution of cluster size and binary properties

The initial half-mass radius of the model clusters is set to be 0.28 pc. The radius increases with time as a result of dynamical relaxation processes. In Fig. 8 we show the evolution of averaged Lagrange radii, radii that contain given enclosed masses. The figure indicates that the central part of the cluster collapses during the first 0.5 Myr, and later expands while outer radii keep increasing. The method we used to create mass-segregated clusters produces more massive stars to be more bound to the cluster, i.e. have lower energy, than lower mass stars. This means that for stars located at the same distance to the cluster centre more massive stars have lower velocities than their lower mass counterparts. However, the kinetic energies of most massive stars in our model are generally higher than those of lower mass stars at a similar distance to the cluster centre because masses of those most massive ( $>30 M_{\odot}$ ) stars are much higher (about 50–80 times) than the average stellar mass in the cluster ( $0.55 M_{\odot}$ ). Thus, even though our models are initially mass segregated in total energy, most massive stars first sink towards the cluster centre at the beginning of the cluster evolution because of dynamical friction.

The averaged half-mass radius expands to  $\approx 0.8$  pc at 5 Myr, almost three times larger than the initial size. After

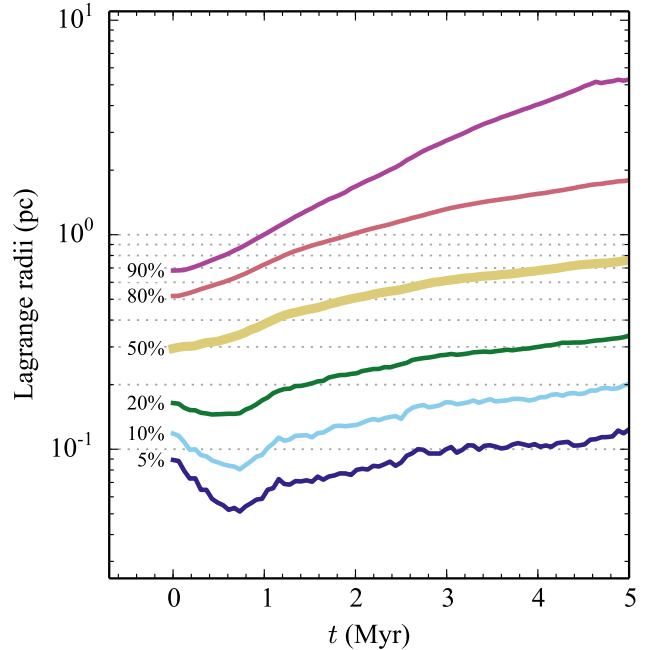


**Figure 8.** Evolution of averaged Lagrange radii. Thick yellow line (50 percent Lagrange radius) is the averaged half-mass radius. Grey dotted lines indicate 0.1, 0.2, ..., 0.9, and 1.0 pc.

a couple of Myr, our model clusters have a comparable size to the observed radius of VVV CL041,  $\approx 0.9 \pm 0.2$  pc (0.75 arcmin at the distance of  $4.2 \pm 0.9$  kpc, Chené et al. 2015).<sup>2</sup>

We note that the size evolution of clusters during the first few Myr is not significantly affected by the initial binary population. For instances, Oh & Kroupa (2012) and Oh et al. (2015) showed that initially single-star clusters and binary-rich clusters have similar half-mass radii at 3 Myr, with a difference of  $\lesssim 0.1$  pc. The evolution of cluster radii over longer time scales is discussed in-depth by Banerjee & Kroupa (2017). The negligible effect of the initial binary population on the dynamical evolution of star clusters has already been noted by Kroupa (1995c).

During cluster evolution, binaries can be disrupted or form through interactions with other binaries and single stars. Figure 9 presents the averaged binary fraction as a function of time for O-type, solar-type and all systems. The binary fraction of all systems represents the value of low-mass binaries because of their large number. A significant fraction of binaries are disrupted within the first Myr, a few crossing times; the half-mass crossing time of our model clusters is  $\approx 0.2$  Myr. The majority of those disrupted binaries are soft binaries of which the initial binding energy,  $|E_b|$ , is lower than the soft-hard-binary boundary,  $\bar{m}\sigma_{\text{cl}}^2/2$  (Fig. 10). As the clusters evolve, the peaks of the evolving distributions move closer to the soft-hard-binary boundary which is  $\log_{10}(|E_b|/M_{\odot} \text{pc}^2 \text{Myr}^{-2}) \approx 0.7$  for our model clusters.

The evolved binary fractions depend on primary mass and are higher for more massive systems. The binary frac-

<sup>2</sup> We note that the observed radius is not the half-mass radius. It is obtained by fitting a King profile adapted to star counts (Chené et al. 2015).



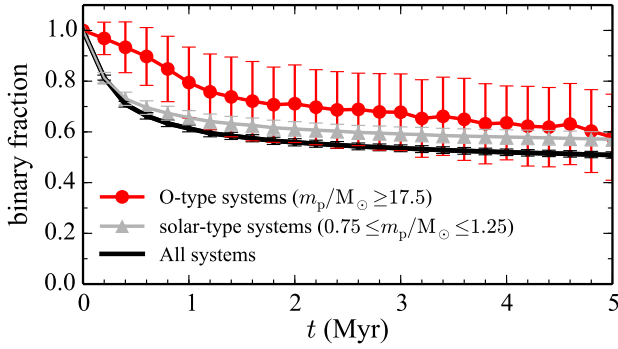


**Figure 9.** Evolution of binary fractions for all (black-), solar-type (grey-), and O-type (red line) systems. The values are averaged for 100 runs and the error bars indicate standard deviation. All systems in the models are counted, i.e. whether they are bound or unbound to the cluster. Only small fraction is unbound thus the values presented are close to the ones for stars that remain in the cluster.

tions at 5 Myr are 0.58, 0.57, and 0.51 for O-type, solar-type, and all systems, respectively. This is because the binary binding energy  $|E_b|$  is higher for more massive stars (Fig. 3) and more massive stars are more likely to form a multiple system dynamically than their lower mass counterparts. For massive binaries which make the high-energy tail, the binary binding energy distribution keeps the initial distribution (small inset figure in Fig. 10). Small differences appear at the low end because of the binary ionisation and at the high end because of stellar collisions. The large dispersion for O-type binaries in Fig. 9 is due to their small number. A model cluster averagely has  $\approx 8$  such systems at the beginning and  $\approx 5$  such systems at 5 Myr.

Most of the binaries removed from the calculations are ionized by stellar interactions. In the meantime a small fraction of binaries become single stars via stellar collisions. In Fig. 11 (bottom) we show averaged initial binding energy distribution of primordial binaries that merge during the first 5 Myr evolution. About half of the binary mergers happen at  $t = 0$  Myr (Fig. 11). They are most energetic binaries among low-mass binaries. Their energy distribution peaks at  $\log_{10}(|E_b|/M_\odot \text{pc}^2 \text{Myr}^{-2}) \approx 2$ . This is 100 times higher energy than the peak of energy distribution of all binaries remain in the cluster,  $\log_{10}(|E_b|/M_\odot \text{pc}^2 \text{Myr}^{-2}) \approx 0$  (Fig. 10). These binaries are low-mass close binaries that are initially on highly eccentric orbit (black triangles in Fig. 11). The mergers are caused by initial configurations that cannot survive during binary formation and should be neglected for study of dynamically induced mergers. For dynamically induced binary mergers, the binding energy distribution is bimodal. A low energy peak appears at  $\log_{10}(|E_b|/M_\odot \text{pc}^2 \text{Myr}^{-2}) \approx 0.2$ , similar to that of binaries remained in the cluster. These merged binaries have high initial eccentricity. Such eccentric binaries have larger encounter cross sections than circular binaries as the binary components stay apocentre for most of time, but also can have a very small separation between binary components. The distribution also peaks at the highest energy  $\log_{10}(|E_b|/M_\odot \text{pc}^2 \text{Myr}^{-2}) \approx 6.2$ . High energy part of the distribution is dominated by massive binaries. The peak appears at about 10 times higher energy than the peak of high-energy

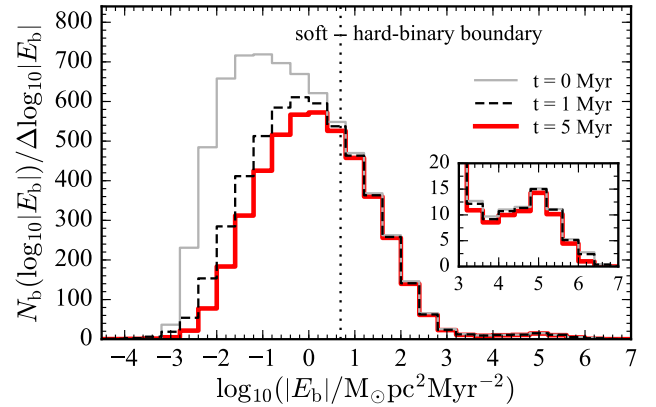


**Figure 10.** Binary binding energy distributions at different times. Grey, black dashed, and red lines are the distributions at 0, 1, and 5 Myr, respectively. In the inset figure, the high-energy tail is zoomed in. The vertical dotted line indicates the soft–hard-binary boundary,  $\bar{m}\sigma_{\text{ecl}}^2/2$ . We note that in this figure the  $Y$ -axis values are numbers of binaries, while those are binary fractions in Fig. 3, to show how many binaries are removed from the calculations, particularly in the high-energy regime.

tail of the binaries that remain in the cluster. For these extremely energetic close binaries, no significant preference of particular eccentricity is shown (top figure of Fig. 11). A number of the initially circular binaries merge for binaries with highest binding energy.

The distribution of orbital parameters is altered by the dynamical processes. Figure 12 presents orbital parameter distributions for O-type ( $m_p \geq 17.5 M_\odot$ ), solar-type ( $0.75 M_\odot \leq m_p \leq 1.25 M_\odot$ ), and all binaries. The distributions for all binaries are dominated by low-mass binaries because of their large number.

For massive binary, a significant fraction of short period binaries are removed within the first 3 Myr. This is due to merging of binaries, likely induced by perturbing systems, rather than ionising of binaries which is the dominant process for long-period binaries. Also a high fraction of mid-long period ( $4 \leq \log_{10}(P/d) \leq 7$ ) binaries disappear during the cluster evolution (Fig. 12). This suggests that those binaries are prone to be involved in dynamical interactions with other systems because of their large separations. The form of the initial mass-ratio distribution (uniform distribution) remains unchanged after the cluster evolution, but low mass-ratio ( $q < 0.1$ ) binaries are formed through dynamical interactions. The eccentricity distribution also keeps its initial shape for the initial eccentricity range ( $0 \leq e \leq 0.6$ ). As a result of close encounters between massive binaries and other massive systems, highly eccentric ( $e > 0.6$ ) binaries are produced.

For solar-type and low-mass systems, the disruptions of binaries occur significantly within the first Myr, a few crossing times, as already mentioned above. Long period binaries are particularly vulnerable to disruption by dynamical interactions because of their large separation (i.e. large cross section) and low binary binding energy  $|E_b|$  (Kroupa 1995b). This is clearly shown in the period distribution of Fig. 12. A large fraction of long period binaries (e.g.  $\log_{10}(P/d) > 5$  for solar-mass binaries) are disrupted while the binary fraction

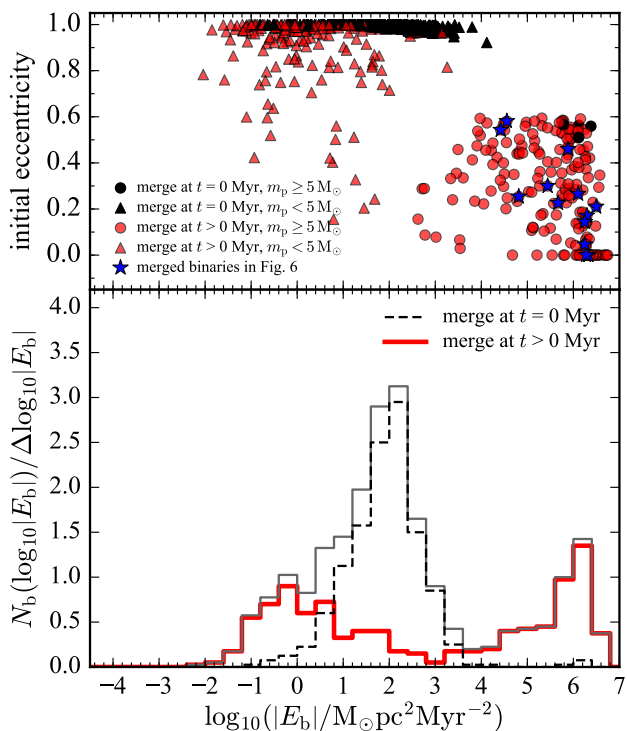


**Figure 11.** Top: initial eccentricity and binding energy of primordial binaries that merge within the first 5 Myr from all 100 calculations. Black and red points are binaries that merge at  $t = 0$  and  $t > 0$  Myr, respectively. Circles are massive binaries ( $m_p \geq 5 M_{\odot}$ ) while triangles are low-mass binaries ( $m_p < 5 M_{\odot}$ ). Blue stars indicate binaries that merge in Fig. 6. Bottom: initial binding energy distribution of the binaries in the top figure. The Y-axis values are averaged numbers in the clusters. The grey line is all binaries that merge within 5 Myr. The black dashed and red thick lines are the binaries that merge at  $t = 0$  and  $t > 0$  Myr, respectively.

of short period binaries remains unchanged. This period-dependent binary-disruption rate results in the dynamically evolved period distribution from our initial distribution to be similar to that of the observed Galactic field solar/low-mass binaries. The mass-ratio distribution evolves through preferred ionisation of binaries with small  $q$  values (Kroupa 1995a). In our models, the mass-ratio distribution of solar-type binaries rises towards smaller  $q$  in agreement with the Duquennoy & Mayor (1991) data but are inconsistent with the flat- $q$  distribution shown in the Raghavan et al. (2010) data. This discrepancy has been discussed in Marks & Kroupa (2011, their section 4.2) and Belloni et al. (2017). We adhere to using the Duquennoy & Mayor (1991) results, notably, because the initial binary population adopted here is in good agreement with a very large range of observational data (Belloni et al. 2017). Note that lack of high- $q$  solar-type binaries in our models compared to the observed distribution (e.g. Duquennoy & Mayor 1991; Raghavan et al. 2010) would disappear with adoption of the eigenevolution process in Kroupa (1995b), which is improved in Belloni et al. (2017). The eccentricity distribution keeps the form of the thermal distribution which is the initial distribution. Overall, different initial conditions for solar/low-mass binary properties do not affect the results concerning the  $m_{\max}-M_{\text{ecl}}$

relation because massive binaries mostly interact with other massive binaries/single-stars.

The dynamical evolution of low-mass/solar-type binaries has been extensively studied (e.g. Kroupa 1995b; Marks & Kroupa 2011; Marks, Kroupa & Oh 2011), while such a study has not been performed for massive binaries. The dynamical processes can alter massive binary populations as well since massive binaries are mostly born in the centre of a cluster (Kirk & Myers 2011; Maschberger & Clarke 2011; Plunkett et al. 2018) where the density is the highest, thus being subject to frequent interactions with other systems. It is worthy to study how dynamical processes affect massive binary populations for constraining their birth distributions and understanding their evolution. But this is beyond the scope of this study. This method of inverse dynamical population synthesis has been used to infer the birth binary distribution functions of  $m_p \leq 1 M_{\odot}$  binaries (Kroupa 1995a,b).

#### 4 DISCUSSION AND SUMMARY

To test the hypothesis that the  $m_{\max}-M_{\text{ecl}}$  relation is valid, it is essential to check if the  $\geq 80 M_{\odot}$  star WR62-2 in the cluster VVV CL041 can be a merger product. Unfortunately, it is very challenging to distinguish whether a star is a merger product or a normal star. The merged star, once formed, evolves as a normal star of the same mass (Suzuki et al. 2007; Glebbeek et al. 2013). Merger products have a larger size and are more luminous than those of normal stars (Glebbeek et al. 2013), though it is unclear how these properties will appear in observation. Merger products of binary systems are also expected to have a high spin and thus to have broadened spectral lines, since the progenitors of a merger are mostly binary components and the angular momentum of the binary orbit will transform to the spin of the merger (e.g. de Mink et al. 2013). However, rapid rotation is not only shown in stellar mergers. Some stars might be born as fast rotators. In addition there are several ways to spin-up massive stars during their evolution in binary or multiple systems, e.g. mass transfer in a binary system (Petrovic, Langer & van der Hucht 2005). We note, in the case of a dynamically induced stellar merger in a high-order multiple system that is likely formed in a dynamical interaction, the merger may not be a fast-rotating star because high-velocity star(s), which can be ejected from the system when merging of the inner binary occurs may carry away the angular momentum. Furthermore, a consequent merger may cancel the stellar spin.

Stellar merger products may be distinguished if the merger products are distinctively younger than the cluster population. Examples are blue stragglers in globular clusters. For star clusters as young as VVV CL041, this may not be easily possible. Rejuvenation by collision appears significant for late-type evolved stars (Schneider et al. 2016), while for young massive stars the rejuvenation would be about  $\leq 1$  Myr which is comparable to their age uncertainty.

If the merger has taken place recently, there may exist gas and dust expelled from the stars during the merging process which may be observable. Indeed, a number of stars have been classified as a merger product from their recent nova and/or the nebula surrounding them, e.g. Mon 838 (Soker & Tylanda 2003; Tylanda & Soker 2006), V1309 Sco

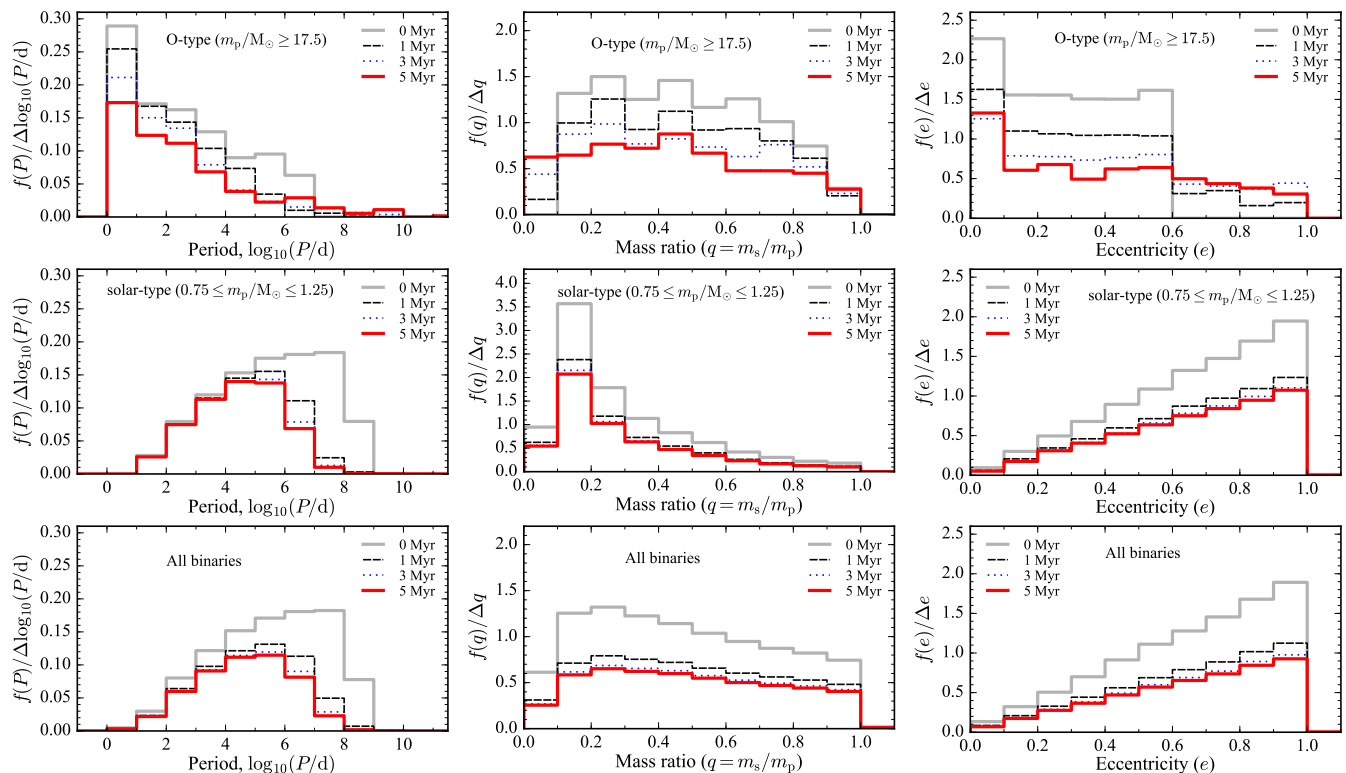


**Figure 12.** Orbital parameter distributions of binaries for O-type (top), solar-type (middle), all (bottom) systems at different times (0, 1, 3, and 5 Myr). From the left to the right, columns are period, mass-ratio, and eccentricity distributions. The area under a histogram equals to the binary fraction (Fig. 9) at a given time for a given stellar type.

(Tylenda et al. 2011; Kamiński et al. 2015b), and CK Vul (Kamiński et al. 2015a). But the gas disperses within a time-scale of 100 000 yr. In particular, if the merger resides in a star cluster, the nebula may disperse more quickly because of the stellar radiation from close massive stars. Older merger might be identified by the B[e] phenomenon (Jeřábková et al. 2016).

We studied whether a moderately massive binary-rich cluster, such as VVV CL041, that initially follows the  $m_{\max} - M_{\text{ecl}}$  relation, can produce a massive star, such as WR62-2 found in the VVV CL041 cluster, via a stellar collision by using direct  $N$ -body calculations with realistic initial conditions. Among 100 direct  $N$ -body calculations, more than 50 per cent of the cluster models form merger products more massive than  $50 M_{\odot}$  during their first 5 Myr of evolution. Furthermore, eight out of 100 clusters form a star more massive than  $80 M_{\odot}$  via multiple collision events. All the merger products involve at least one primordial massive binary. Our results suggest that the VVV CL041 cluster would have been initially on the  $m_{\max} - M_{\text{ecl}}$  relation, and that its present-day most massive star, WR62-2, may be a merger product. It will be fruitful to also study, in the future, the occurrence of less massive mergers in such realistic  $N$ -body models.

We show that clusters can have their most massive star deviating from the  $m_{\max} - M_{\text{ecl}}$  relation even if the cluster was initially on the relation. We note that a single or even a few cases of clusters that appear to violate the relation cannot, in fact, rule out the existence of the relation. The dynamical history of a star cluster varies from cluster to cluster and

we capture snapshots by observation of star clusters at 1 to few Myr after they form. There, thus, likely exist outliers that resulted from the here quantified evolutionary processes even though they initially follow the relation. With a large sample of star clusters, as shown in Weidner et al. (2013) and in the recent homogeneous survey of young star clusters presented in Ramírez Alegría et al. (2016), Kirk & Myers (2011), and Stephens et al. (2017), the  $m_{\max} - M_{\text{ecl}}$  relation appears to be well established (Fig. 1), but further critical study of this potentially fundamentally-important relation is needed.

## ACKNOWLEDGMENTS

We are very grateful to Sverre Aarseth for making his NBODY6 freely available and continuing its improvements. We thank our referee Ian Bonnell for his constructive comments that improved our manuscript. SO thanks her husband Joachim Bestenlehner for his support and her newborn son Nuri Bestenlehner for his cooperation when the last revision was made. This research has made use of NASA’s Astrophysics Data System Bibliographic Services.

## REFERENCES

- Aarseth S. J., 2003, *Gravitational N-Body Simulations*. Cambridge: Cambridge Univ. Press  
 Banerjee S., Kroupa P., 2017, *A&A*, **597**, A28

- Banerjee S., Kroupa P., Oh S., 2012, *MNRAS*, **426**, 1416
- Baumgardt H., De Marchi G., Kroupa P., 2008, *ApJ*, **685**, 247
- Belloni D., Askar A., Giersz M., Kroupa P., Rocha-Pinto H. J., 2017, *MNRAS*, **471**, 2812
- Brinkmann N., Banerjee S., Motwani B., Kroupa P., 2017, *A&A*, **600**, A49
- Chené A.-N., et al., 2015, *A&A*, **584**, A31
- Duquennoy A., Mayor M., 1991, *A&A*, **248**, 485
- Elmegreen B. G., 2006, *ApJ*, **648**, 572
- Gaburov E., Gualandris A., Portegies Zwart S., 2008, *MNRAS*, **384**, 376
- Glebbeeck E., Gaburov E., Portegies Zwart S., Pols O. R., 2013, *MNRAS*, **434**, 3497
- Goodwin S. P., Kroupa P., 2005, *A&A*, **439**, 565
- Heggie D., Hut P., 2003, *The Gravitational Million-Body Problem: A Multidisciplinary Approach to Star Cluster Dynamics*. Cambridge Univ. Press, Cambridge
- Hills J. G., Day C. A., 1976, *Astrophys. Lett.*, **17**, 87
- Hurley J. R., Pols O. R., Tout C. A., 2000, *MNRAS*, **315**, 543
- Hurley J. R., Tout C. A., Pols O. R., 2002, *MNRAS*, **329**, 897
- Jeřábková T., et al., 2016, *A&A*, **586**, A116
- Kamiński T., Menten K. M., Tylanda R., Hajduk M., Patel N. A., Kraus A., 2015a, *Nature*, **520**, 322
- Kamiński T., Mason E., Tylanda R., Schmidt M. R., 2015b, *A&A*, **580**, A34
- Kiminki D. C., Kobulnicky H. A., 2012, *ApJ*, **751**, 4
- Kirk H., Myers P. C., 2011, *ApJ*, **727**, 64
- Kirk H., Myers P. C., 2012, *ApJ*, **745**, 131
- Kobulnicky H. A., et al., 2014, *ApJS*, **213**, 34
- Kroupa P., 1995a, *MNRAS*, **277**, 1491
- Kroupa P., 1995b, *MNRAS*, **277**, 1507
- Kroupa P., 1995c, *MNRAS*, **277**, 1522
- Kroupa P., 2008, in Aarseth S. J., Tout C. A., Mardling R. A., eds, *Lecture Notes in Physics Vol. 760, The Cambridge N-Body Lectures*. Berlin: Springer, p. 181 ([arXiv:0803.1833](https://arxiv.org/abs/0803.1833)), [doi:10.1007/978-1-4020-8431-7\\_8](https://doi.org/10.1007/978-1-4020-8431-7_8)
- Kroupa P., Aarseth S., Hurley J., 2001, *MNRAS*, **321**, 699
- Kroupa P., Weidner C., Pflamm-Altenburg J., Thies I., Dabringhausen J., Marks M., Maschberger T., 2013, in Oswald T. D., Gilmore G., eds, *Planets, Stars and Stellar Systems. Volume 5: Galactic Structure and Stellar Populations*. Dordrecht: Springer, p. 115, [doi:10.1007/978-94-007-5612-0\\_4](https://doi.org/10.1007/978-94-007-5612-0_4)
- Leonard P. J. T., 1989, *AJ*, **98**, 217
- Leonard P. J. T., Duncan M. J., 1988, *AJ*, **96**, 222
- Lombardi Jr. J. C., Rasio F. A., Shapiro S. L., 1996, *ApJ*, **468**, 797
- Maíz Apellániz J., et al., 2015, *A&A*, **579**, A108
- Marks M., Kroupa P., 2011, *MNRAS*, **417**, 1702
- Marks M., Kroupa P., 2012, *A&A*, **543**, A8
- Marks M., Kroupa P., Oh S., 2011, *MNRAS*, **417**, 1684
- Maschberger T., Clarke C. J., 2011, *MNRAS*, **416**, 541
- Oh S., Kroupa P., 2012, *MNRAS*, **424**, 65
- Oh S., Kroupa P., 2016, *A&A*, **590**, A107
- Oh S., Kroupa P., Pflamm-Altenburg J., 2015, *ApJ*, **805**, 92
- Petrovic J., Langer N., van der Hucht K. A., 2005, *A&A*, **435**, 1013
- Plunkett A. L., Fernández-López M., Arce H. G., Busquet G., Mardones D., Dunham M. M., 2018, *A&A*, **615**, A9
- Portegies Zwart S. F., McMillan S. L. W., Gieles M., 2010, *ARA&A*, **48**, 431
- Raghavan D., et al., 2010, *ApJS*, **190**, 1
- Ramírez Alegría S., et al., 2016, *A&A*, **588**, A40
- Rauw G., Sana H., Antokhin I., Morrell N., Niemela V., Colombo J. A., Gosset E., Vreux J.-M., 2001, *Monthly Notices of the Royal Astronomical Society*, **326**, 1149
- Sana H., et al., 2012, *Science*, **337**, 444
- Sana H., et al., 2014, *ApJS*, **215**, 15
- Schneider F. R. N., Podsiadlowski P., Langer N., Castro N., Fosfari L., 2016, *MNRAS*, **457**, 2355
- Schulz C., Pflamm-Altenburg J., Kroupa P., 2015, *A&A*, **582**, A93
- Selman F. J., Melnick J., 2008, *ApJ*, **689**, 816
- Sills A., Faber J. A., Lombardi Jr. J. C., Rasio F. A., Warren A. R., 2001, *ApJ*, **548**, 323
- Soker N., Tylanda R., 2003, *ApJ*, **582**, L105
- Stephens I. W., et al., 2017, *ApJ*, **834**, 94
- Suzuki T. K., Nakasato N., Baumgardt H., Ibukiyama A., Makino J., Ebisuzaki T., 2007, *ApJ*, **668**, 435
- Testi L., Palla F., Prusti T., Natta A., Maltagliati S., 1997, *A&A*, **320**, 159
- Tylanda R., Kamiński T., 2016, *A&A*, **592**, A134
- Tylanda R., Soker N., 2006, *A&A*, **451**, 223
- Tylanda R., et al., 2011, *A&A*, **528**, A114
- Weidner C., Kroupa P., Pflamm-Altenburg J., 2013, *MNRAS*, **434**, 84
- Yan Z., Jerabkova T., Kroupa P., 2017, *A&A*, **607**, A126
- de Mink S. E., Langer N., Izzard R. G., Sana H., de Koter A., 2013, *ApJ*, **764**, 166

This paper has been typeset from a  $\text{\TeX}/\text{\LaTeX}$  file prepared by the author.